Available online at www.sciencedirect.com
ScienceDirect
Journal of Nuclear Materials 363–365 (2007) 1261–1265
journal of nuclear materials
www.elsevier.com/locate/jnucmat

Parametric studies of carbon erosion mitigation dynamics in beryllium seeded deuterium plasmas

D. Nishijima *, M.J. Baldwin, R.P. Doerner, R. Seraydarian

Center for Energy Research, University of California at San Diego, 9500 Gilman Dr., La Jolla, CA 92093-0417, USA

Abstract

The characteristic time of protective beryllium layer formation on a graphite target, $\tau_{Be/C}$, has been investigated as a function of surface temperature, T_s, ion energy, E_i, ion flux, Γ_i, and beryllium ion concentration, c_{Be}, in beryllium seeded deuterium plasma. $\tau_{Be/C}$ is found to be strongly decreased with increasing T_s in the range of 550–970 K. This is thought to be associated with the more efficient formation of beryllium carbide (Be_2C). By scanning the parameters, a scaling expression for $\tau_{Be/C}$ has been derived as $\tau_{Be/C}[s] = 1.0 \times 10^{-7} c_{Be}^{-1.9\pm0.1} E_i^{0.9\pm0.3} \Gamma_i^{-0.6\pm0.3} \exp((4.8 \pm 0.5) \times 10^3/T_s)$, where c_{Be} is dimensionless, E_i in eV, Γ_i in 10^{22} m^{-2} s^{-1} and T_s in K. Should this scaling extend to an ITER scenario, carbon erosion of the divertor strike point region may be reduced with characteristic time of ~6 ms. This is much shorter than the time between predicted ITER type I ELMs (~1 s), and suggests that protective beryllium layers can be formed in between ELMs, and mitigate carbon erosion.

PACS: 52.40.Hf

Keywords: PISCES-B; Beryllium; Carbon; Mixed-material; Chemical erosion

1. Introduction

Mixed-material effects have attracted great interest since ITER will have beryllium, carbon and tungsten as plasma facing components (PFCs). Beryllium sputtered from the first wall is expected to migrate to the divertor region, where the strike point region is made of carbon material. Tungsten is used in the baffle region. Since the beryllium concentration in the divertor plasma is predicted to be in the range of 0.01–0.1, interaction of beryllium with carbon and tungsten materials may change the original properties of those materials.

Previous experiments [1,2] on beryllium/carbon mixed-material effects in the linear divertor plasma simulator PISCES-B revealed that both chemical and physical erosion of carbon was mitigated by beryllium impurities in the plasma. This was identified by a reduction of CD ($A^2\Delta - X^2\Pi$) band intensity and C I line intensity. X-ray photoelectron spectroscopy (XPS) analyses of these targets subsequent to plasma exposure revealed the formation of beryllium carbide (Be_2C), which is thought to play an important role in carbon erosion mitigation. Work on beryllium/tungsten mixed-material effects

* Corresponding author. Fax: +1 858 534 7716.
E-mail address: dnishijima@ferp.ucsd.edu (D. Nishijima).

0022-3115/$ - see front matter © 2007 Elsevier B.V. All rights reserved.
doi:10.1016/j.jnucmat.2007.01.177

has been also performed in PISCES-B, and is reported in these proceedings [3].

In this paper we extend previous work [2] on carbon erosion mitigation in beryllium seeded deuterium plasma. In Ref. [2], the dependence of the protective beryllium layer formation time, $\tau_{Be/C}$, on beryllium ion concentration, c_{Be}, was investigated. Here, we reveal further dependence of $\tau_{Be/C}$ on other parameters, such as incident ion energy, E_i, surface temperature, T_s, and incident ion flux, Γ_i. A scaling law for $\tau_{Be/C}$ is derived from a regression analysis of the data and this scaling is used to predict carbon erosion behavior under ITER divertor relevant conditions.

2. Experimental setup

Experiments are performed in the linear divertor plasma simulator PISCES-B [4], which produces a high flux (up to $10^{23}\,m^{-2}\,s^{-1}$) steady state plasma. ATJ graphite targets, 22 mm in diameter and 2.8 mm thick, are exposed to beryllium seeded deuterium plasmas. Beryllium impurities are injected into the plasma column using a high-temperature effusion cell (Veeco Applied EPI), located at ~150 mm upstream from the target as shown in Fig. 1. The amount of beryllium impurities can be controlled by varying the temperature of effusion cell. The injected beryllium atoms are ionized in the plasma and transported to the target. The singly ionized beryllium density, n_{Be+}, in the plasma is obtained from Be II ($\lambda = 467.3$ nm) line intensity measured with an absolutely calibrated spectroscopic system. The necessary photon emission coefficient is taken from the ADAS database [5]. The electron density, n_e, the electron temperature, T_e, and the ion flux, Γ_i, are measured with a fast scanning double probe system at the same axial position as the effusion cell. The incident ion energy, E_i, is controlled by biasing the target with a negative potential relative to the plasma potential. The sample temperature is measured with a thermocouple contacted to the back side of target.

3. Measuring $\tau_{Be/C}$

The characteristic time of protective beryllium layer formation on a graphite sample, in other words, the carbon erosion mitigation time, $\tau_{Be/C}$, is determined from the decay of CD ($A^2\Delta - X^2\Pi$) band intensity around λ ~430 nm as shown in Fig. 2. In Ref. [2], the CD band intensity decay is found to correlate closely with beryllium layer formation on a graphite sample. At $t = 0$ s, beryllium is injected into the plasma by opening the shutter of the effusion cell. During the exposure, the D_γ intensity is fairly constant, indicating that the plasma conditions are unchanged. The subtraction of CD band intensity taken in a region far from the target (~70 mm upstream) is used to eliminate the effects of the intensity originating from wall carbon erosion [2,6]. From the exponential fit, $\tau_{Be/C}$ is derived in this example to be around 83 s.

4. Individual parameter dependence of $\tau_{Be/C}$

In Fig. 3, $\tau_{Be/C}$ is plotted as a function of beryllium ion concentration in the plasma, $c_{Be} = n_{Be+}/n_e$.

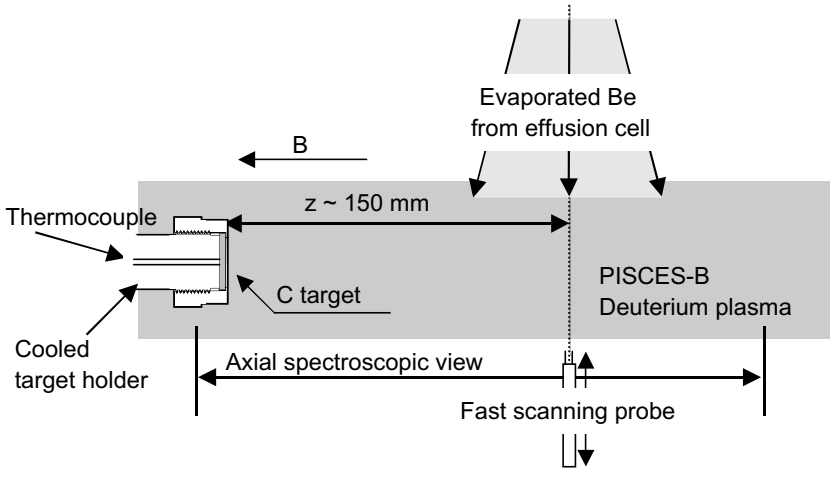

Fig. 1. Schematic view of the target region in the linear divertor plasma simulator PISCES-B. A graphite target is exposed to a beryllium seeded deuterium plasma.

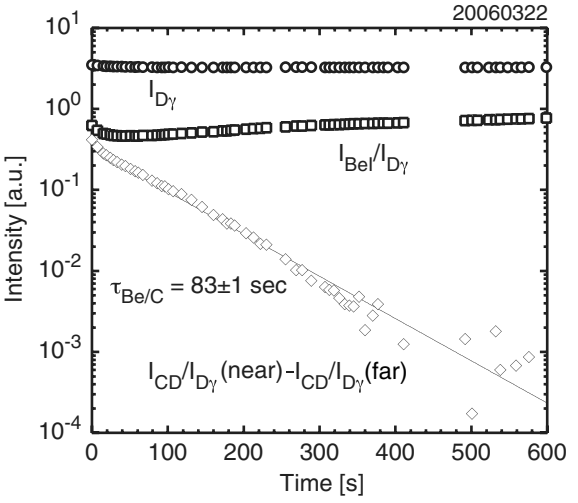

Fig. 2. Time evolution of D_γ, normalized Be I (457.3 nm) and CD ($A^2\Delta - X^2\Pi$) band intensity near the target during a beryllium seeded deuterium plasma exposure of a graphite target ($c_{Be} \sim 1.3 \times 10^{-3}$, $T_s \sim 800$ K, $E_i \sim 34$ eV, $\Gamma_i \sim 3.5 \times 10^{22}$ m^{-2} s^{-1}). The CD band intensity taken in a region far from the target is subtracted from that near the target to eliminate changes in the CD band intensity originating from wall carbon erosion.

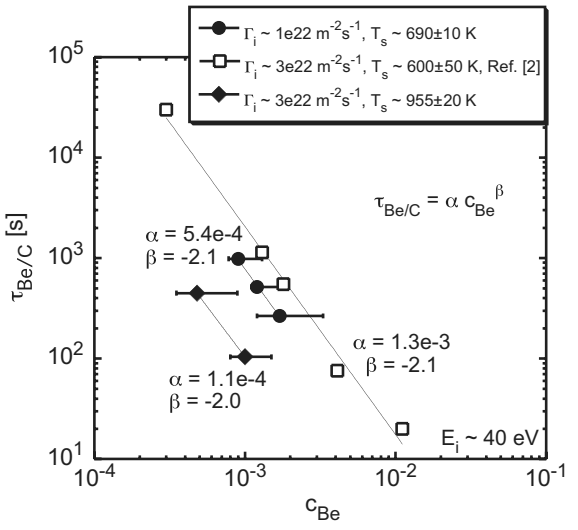

Fig. 3. Beryllium ion concentration, c_{Be}, dependence of $\tau_{Be/C}$ at three different conditions with E_i of ~40 eV. Circles: $\Gamma_i \sim 1 \times 10^{22}$ m^{-2} s^{-1}, $T_s \sim 690 \pm 10$ K, Squares: $\Gamma_i \sim 3 \times 10^{22}$ m^{-2} s^{-1}, $T_s \sim 600 \pm 50$ K [2], Diamonds: $\Gamma_i \sim 3 \times 10^{22}$ m^{-2} s^{-1}, $T_s \sim 955 \pm 20$ K. Lines show results of power function fits ($\tau_{Be/C} = \alpha\, c_{Be}^{\beta}$), revealing $\beta \sim -2$.

In this data set, E_i, T_s and Γ_i are kept constant for three different plasma regimes. As reported in Ref. [2], the higher c_{Be} leads to the shorter $\tau_{Be/C}$, where a power function fit, $\tau_{Be/C} = \alpha\, c_{Be}^{\beta}$, gives $\beta \sim -2$. The additional data confirm the c_{Be} dependence of $\tau_{Be/C}$

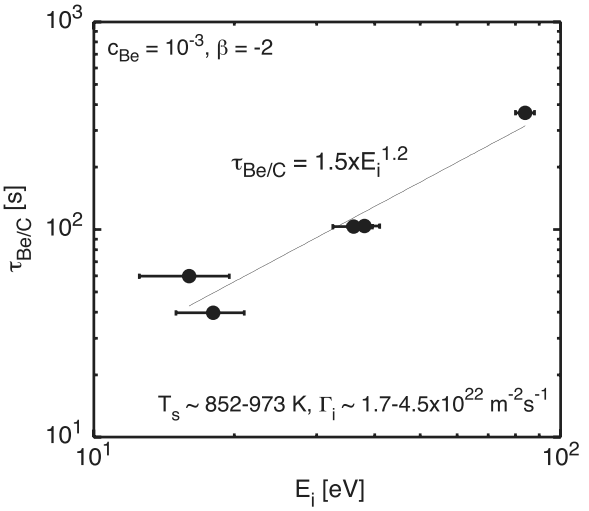

Fig. 4. Incident ion energy, E_i, dependence of $\tau_{Be/C}$. To compensate the c_{Be} dependence, $\tau_{Be/C}$ is calculated at $c_{Be} = 10^{-3}$ with $\beta = -2$ in the power law, $\tau_{Be/C} = \alpha\, c_{Be}^{\beta}$, from measured data.

at different Γ_i and T_s that were not investigated in Ref. [2].

Fig. 4 shows the dependence of $\tau_{Be/C}$ on E_i for the chosen value of $c_{Be} = 10^{-3}$ by assuming $\beta = -2$ in the power law, $\tau_{Be/C} = \alpha\, c_{Be}^{\beta}$ to compensate the c_{Be} dependence. The dependence on T_s and Γ_i is not compensated. It is found from Fig. 4 that $\tau_{Be/C}$ increases with E_i, at least up to ~85 eV. This tendency can be qualitatively explained by the fact that beryllium deposited on the graphite target can be more readily sputtered at higher E_i, thus resulting in a longer $\tau_{Be/C}$. It should be noted that the sputtering yield of

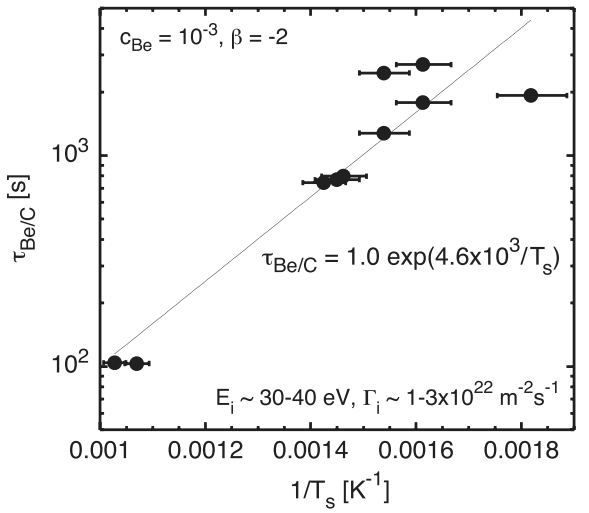

Fig. 5. Surface temperature, T_s, dependence of $\tau_{Be/C}$. Similarly, $\tau_{Be/C}$ is derived at $c_{Be} = 10^{-3}$ with $\beta = -2$ from measured data.

polycrystalline beryllium by deuterium ions has a maximum at around 200 eV [7], although the sputtering yield of beryllium deposited on graphite material is not available.

As shown in Fig. 5, where $\tau_{Be/C}$ is similarly calculated at $c_{Be} = 10^{-3}$ with $\beta = -2$ from measured data, $\tau_{Be/C}$ is found to strongly depend on T_s. At a higher T_s of ~950 K ($1/T_s \sim 0.001\ K^{-1}$), $\tau_{Be/C}$ is shorter than that at $T_s \sim 600$ K ($1/T_s \sim 0.0017\ K^{-1}$) by a factor of ~20. This observation is qualitatively consistent with XPS analyses of graphite samples exposed to beryllium seeded deuterium plasmas at several different T_s [8]. Namely, the higher T_s leads to increased reaction of the beryllium and carbon, resulting in full surface carbidisation with Be_2C.

An Arrhenius exponential function is used to fit the surface temperature dependent data since a surface reaction rate, K, is generally described by an exponent of a ratio of the enthalpy of formation, ΔH_{298}, to T_s. The enthalpy of formation of Be_2C, $\Delta H_{298}(Be_2C)$, is reported as -117.0 ± 1.0 kJ/mol [9], giving the Be_2C formation time as, $\tau_{Be_2C} \propto 1/K_{Be_2C} \propto \exp(1.4e4/T_s)$. The numerator in the exponential function is around 3 times larger than that in the protective beryllium layer formation time, $\tau_{Be/C} \propto \exp(4.6e3/T_s)$, derived from the experiments, meaning that $\tau_{Be/C}$ has a weaker T_s dependence than τ_{Be_2C}. This implies the following:

- Pure beryllium layers on Be_2C also contributes to the carbon erosion reduction especially at lower T_s. Actually, XPS analyses show coexistence of elemental beryllium and Be_2C at lower T_s [8]. And/or
- $\Delta H_{298}(Be_2C)$ may be lower in the plasma-material interaction environment than the equilibrium value reported in the literature.

Ashida et al. [10] performed an experiment, where a carbon film was deposited on a beryllium plate by rf discharge of C_2H_4, subsequently the sample was heated up at given temperatures. An Arrhenius plot of the $Be_2C(1\,1\,1)$ peak intensity measured with X-ray diffractometry (XRD) gives a value of around 5000 K for the numerator in the exponential function, which is interestingly very close to our value.

5. Scaling expression for $\tau_{Be/C}$ and extrapolation to ITER condition

Given the experimentally determined parametric forms, a regression analysis was performed with the parameters, c_{Be}, E_i, T_s and Γ_i to obtain a scaling law for $\tau_{Be/C}$. In Fig. 6 the experimentally derived $\tau_{Be/C}$ is compared with the scaling expression

$$\tau^{scale}_{Be/C}[s] = 1.0 \times 10^{-7} c_{Be}^{-1.9\pm0.1} E_i^{0.9\pm0.3} \Gamma_i^{-0.6\pm0.3} \times \exp((4.8 \pm 0.5) \times 10^3/T_s), \quad (1)$$

where $c_{Be} = n_{Be+}/n_e$ is dimensionless, E_i in eV, Γ_i in $10^{22}\ m^{-2}\ s^{-1}$ and T_s in K. Each parameter scan range is shown in the figure. The experimental values are found to agree well with the scaling law. Note that the exponent of each parameter is slightly different from that shown in the previous section since in the individual parameter scan (Figs. 3–5) the dependence on other parameters are not precisely taken into account while the c_{Be} dependence is compensated by using $\beta = -2$.

It is found from the scaling law that $\tau_{Be/C}$ has a negative power law dependence on Γ_i, i.e. higher Γ_i leads to quicker beryllium layer formation. This is because the redeposited fraction of sputtered beryllium atoms is increased due to the higher ionization rate of sputtered beryllium atoms at higher Γ_i.

Although some of typical values for the parameters expected in the ITER divertor carbon targets are outside our scanned ranges, the scaling law can be used to predict the protective beryllium layer formation time in the ITER situation. With $c_{Be} = 0.05$, $E_i = 20$ eV, $T_s = 1200$ K and $\Gamma_i = 10^{23}\ m^{-2}\ s^{-1}$ [11], the scaling expression gives $\tau_{Be/C} \sim$ 6 ms, which is much shorter than a

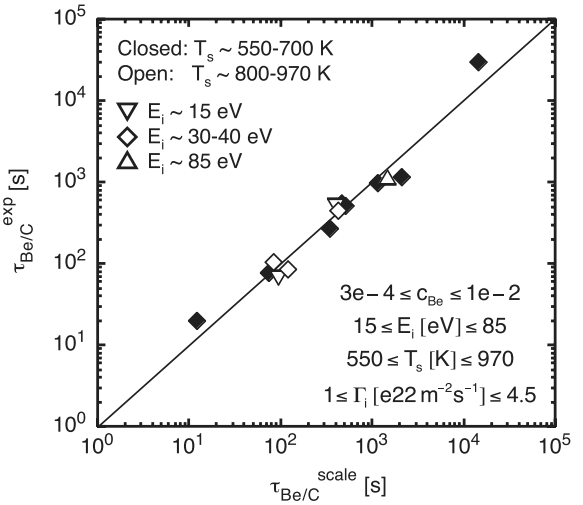

Fig. 6. Comparison of experimental protective beryllium layer formation time, $\tau^{exp}_{Be/C}$, with the scaling expression in Eq. (1).

predicted ITER type I ELM period, i.e. the inverse of ELM frequency, of ~1 s [12]. This suggests that protective beryllium layers on carbon targets can be formed in between ELMs, thereby reducing the carbon erosion during the period between ELMs.

6. Conclusion

We have derived a scaling expression for the characteristic formation time of protective beryllium layer on a graphite sample from parametric scan experiments in beryllium seeded deuterium plasmas of the PISCES-B linear divertor simulator. The scaling expression is in good agreement with the experimentally derived beryllium layer formation time. The predicted formation time in a typical ITER divertor condition is found to be much shorter than the inverse of expected ITER type I ELM frequency of ~1 Hz. This result is favorable for mitigating carbon erosion. We plan to extend the experimental parameter ranges to increase confidence in the scaling law.

Acknowledgements

The authors express their sincere thanks to PISCES technical staff for their professional skill and dedication. Discussion with PISCES scientific members was really fruitful. This work is conducted under the US Department of Energy Contract: DOE DE-FG03-95ER-54301.

References

[1] R.P. Doerner et al., in: Proc. 20th IAEA Fus. Ener. Conf., Vilamoura, Portugal, 2004, p. IT/P3-18.
[2] M.J. Baldwin, R.P. Doerner, Nucl. Fusion 46 (2006) 444.
[3] M.J. Baldwin et al., J. Nucl. Mater., these Proceedings, doi: 10.1016/j.jnucmat.2007.01.151.
[4] R.P. Doerner et al., Phys. Scripta T111 (2004) 75.
[5] H.P. Summers, Atomic Data and Analysis Structure-User Manual, Report JET-IR(94), JET Joint Undertaking, Abingdon, 1994.
[6] D.G. Whyte et al., Nucl. Fusion 41 (2001) 47.
[7] W. Eckstein, Calculated Sputtering, Reflection and Range Values, Rep. IPP 9/132 Max-Planck-Institut für Plasmaphysik, Garching, 2002.
[8] M.J. Baldwin et al., J. Nucl. Mater. 358 (2006) 96.
[9] O. Kubaschewski et al., Materials Thermo-chemistry, 6th Ed., Pegamon, Oxford, 1993.
[10] K. Ashida et al., J. Nucl. Mater. 241–243 (1997) 1060.
[11] G. Federici et al., J. Nucl. Mater. 266–269 (1999) 14.
[12] G. Federici et al., Plasma Phys. Contr. Fusion 45 (2003) 1523.